Electronic state spectroscopy of C_2Cl_4

Journal Item

Electronic State Spectroscopy of C_2Cl_4

S. Eden, B. Barc, N.J. Mason, S.V. Hoffmann, Y. Nunes, P. Limão-Vieira

PII: S0301-0104(09)00312-7
DOI: 10.1016/j.chemphys.2009.10.010
Reference: CHEMPH 7752

To appear in: *Chemical Physics*

Received Date: 9 June 2009
Accepted Date: 8 October 2009

Please cite this article as: S. Eden, B. Barc, N.J. Mason, S.V. Hoffmann, Y. Nunes, P. Limão-Vieira, Electronic State Spectroscopy of C_2Cl_4, *Chemical Physics* (2009), doi: 10.1016/j.chemphys.2009.10.010

Electronic State Spectroscopy of C_2Cl_4

S. Eden [1,2*], B. Barc [1], N.J. Mason [1], S.V. Hoffmann [3], Y. Nunes [4], and P. Limão-Vieira [1, 4]

[1] *Dept. of Physics and Astronomy, Open University, Walton Hall, Milton Keynes MK7 6AA, UK*
[2] Also of *Institut de Physique Nucléaire de Lyon, IN2P3-CNRS et Université Claude Bernard Lyon 1, 43, boulevard du 11 Novembre 1918, 69622 Villeurbanne Cedex, France*
[3] *Institute of Storage Rings, University of Aarhus, Ny Munkegade, Aarhus, Denmark*
[4] *Laboratório de Colisões Atómicas e Moleculares, CEFITEC, Departamento de Física, FCT - Universidade Nova de Lisboa, P-2829-516 Caparica, Portugal*

Abstract

The VUV spectrum of C_2Cl_4 is reported in the energy range 3.8-10.8 eV (325-115 nm). Several photoabsorption features are observed for the first time, including a very weak low-lying band which is provisionally attributed to a $\pi \rightarrow \pi^*$ triplet transition. Recent *ab initio* calculations of the molecule's electronic transitions [Arulmozhiraja et al. *J. Chem. Phys.* 129 (2008) 174506] provide the basis for the present assignments below 8.5 eV. An extended *n*dπ series is proposed to account for several higher-energy Rydberg bands. The identification of vibrational structure, dominated by symmetric C=C and CCl_2 stretching in excitations from the HOMO, largely agrees with previous spectroscopic studies. The present absolute photoabsorption cross sections cover a wider energy range than the previous measurements and are used to calculate UV photolysis *lifetimes* of this aeronomic molecule at altitudes between 20 and 50 km.

Key Words

Photoabsorption; C_2Cl_4; tetrachloroethylene; electronic excitation; vibrational excitation; Rydberg series; photolysis

Classifications

10.150 Molecular spectroscopy, UV
10.300 Synchrotron spectroscopies
40.120 Molecules (neutral and ionic)
50.080 Electronic structure and states
50.160 Ionization (incl. Rydberg states)
50.480 Vibrations and rotations of molecules

* Corresponding author s.p.eden@open.ac.uk

1. Introduction

As a halogenated atmospheric gas with no known natural sources, tetrachloroethylene (C_2Cl_4) has been the subject of various studies focusing on the environmental effects of industrial emissions [1-4]. In particular, the compound is used extensively as a dry-cleaning solvent and a degreasing agent. Indeed its dispersion has been studied as a tracer for urban/industrial activities [5]. The UV photoabsorption spectrum and absolute cross sections can be used to monitor the concentration of C_2Cl_4 molecules in various industrial and atmospheric contexts, while its electronic state spectroscopy provides key insights into photo-induced dissociation with applications in modeling gas-phase chemistries. Accordingly, the present absolute cross sections for the broad absorption band dominated by the dissociative $\pi(C=C) \rightarrow \pi^*(C=C)$ transition have been used to calculate solar UV photolysis rates at altitudes from 20 to 50 km (section 4.3). As a source of Cl and CCl_2 radicals, stratospheric C_2Cl_4 can contribute to ozone depletion. Indeed Kindler et al. [1] have reported an ozone depletion potential (ODP, relative to CF_3Cl) for C_2Cl_4 of $\sim 6\times10^{-3}$, similar to the more abundant CH_3Cl.

UV photoabsorption by C_2Cl_4 has been studied on several previous occasions [6-11]. In addition, Koerting et al. [12] have carried out electron scattering experiments probing its singlet and triplet excited states, while semi-empirical self-consistent field molecular orbital (SCF MO) calculations have been performed by Kato et al. [13]. The molecule's multi-photon ionization spectroscopy has been studied in detail by Williams and co-workers [14,15]. However, prior to Arulmozhiraja et al.'s [16] recent work, no *ab initio* calculations of the single-photon absorption electronic transitions (energies and oscillator strengths) were available to support the UV spectral assignments. In the present work, it has therefore been possible to draw upon advanced theoretical calculations for the first time in order to interpret the electronic state spectroscopy of C_2Cl_4 below the lowest ionization energy.

2. Brief review of the geometry and electronic configuration of C_2Cl_4

The valence shell molecular orbital configuration of C_2Cl_4 in the electronic ground state (^1A_g) can be represented as $\ldots(2b_{3g})^2\ (9a_g)^2\ (8b_{1u})^2\ (2b_{1g})^2\ (7b_{3u})^2\ (2a_u)^2\ (7b_{2g})^2\ (3b_{2u})^2$ with D_{2h} symmetry [17]. The highest occupied molecular orbital (HOMO) has been identified as having $\pi(C=C)$ character. In contrast with the HOMO of ethylene and tetrafluoroethylene, C_2F_4, which are entirely C=C localized [18], the C_2Cl_4 HOMO has been reported to be partially delocalized over the chlorine atoms [19,20]. The geometry of tetrachloroethylene is represented schematically as an insert in figure 1. The vibrational modes and excitation energies of the molecule in the neutral electronic ground state are listed in table 1 [21].

On the basis of the convergence of Rydberg series observed by REMPI spectroscopy, Williams et al. [14] determined the lowest adiabatic ionization energy (AIE) of C_2Cl_4 to be 9.3256 ± 0.0006 eV. This value is in close agreement with AIE derived from Lake and Thompson's [22] photoelectron experiments. In the present work, Lias' [23] *evaluated* AIE of 9.326 ± 0.001 eV has been used to calculate quantum defects associated with transitions from the HOMO to Rydberg orbitals (section 4.2.1).

The ionic states of C_2Cl_4 below 20 eV are summarized in table 2. The photoelectron bands between 11 and 14 eV have been assigned to electron emission from essentially non-bonding Cl atomic orbitals [20,22]. The photoelectron data is generally in good agreement with the most recent calculations [17], while only the highest energy n(Cl) band (13.48 eV) showed experimental evidence for vibrational excitation (symmetric C-Cl stretching, ν_2). The lack of vibrational features in the bands reported above 14 eV suggests further n(Cl) bands or dissociative ionization; possibly due to the vacation of strongly bonding σ MOs. Accordingly, Kimura et al. [20] attributed these bands to electron emission from orbitals of predominantly σ(C-Cl), σ(C-C), and n(Cl) character on the basis of self-consistent field (SCF) calculations, while

electron impact ionization experiments have shown the appearance energy of CCl_2^+ to be 14.7 eV [24].

3. Experimental

The present photoabsorption measurements were made at the ASTRID facility, Aarhus University, Denmark. The experimental apparatus has been described in detail elsewhere [25]. Briefly, synchrotron radiation passes through a static gas sample (LiF entrance window and CaF_2 exit) and a photomultiplier is used to measure the transmitted light intensity. The incident wavelength is selected using a toroidal dispersion grating with 2000 lines/mm providing a resolution of 0.075 nm, corresponding to 3 meV at the midpoint of the energy range studied. For wavelengths below 200 nm (energies above 6.20 eV), helium is flushed through the small gap between the photomultiplier and the exit window of the gas cell to prevent any absorption by air contributing to the spectrum. Measurements are carried out at 298±1 K and the sample pressure is measured using a capacitance manometer (Baratron). To ensure that the data is free of any saturation effects, absorption cross sections are recorded over the pressure range 0.001 – 1.0 mbar, with typical attenuations of less than 10%. The synchrotron beam ring current is monitored throughout the collection of each spectrum and background scans are recorded with the cell evacuated. Absolute photoabsorption cross sections are then obtained using the Beer-Lambert attenuation law:

$$I_t = I_0 \exp(-n\sigma x) \qquad \text{[eq. 1]}$$

where I_t is the radiation intensity transmitted through the gas sample, I_0 is that through the evacuated cell, n the molecular number density of the sample gas, σ the absolute photoabsorption cross section, and x the absorption path length (25.0 cm).

SO_2 was used to calibrate the energy scale since it has clearly defined sets of sharp absorption peaks from 3.8 to 5.1 eV [26] and from 5.15 to 7.25 eV [27]. The energy resolution for the present results is calculated to be 0.07 nm, corresponding to 3 meV at the midpoint of the energy range studied. The error on the absolute cross section measurements is estimated at ± 5% [25,28]. Only when absorption by the sample is very weak ($I_o \approx I_t$), does the error increase significantly as a percentage of the measured cross section.

The liquid C_2Cl_4 sample (boiling point 121.1 °C [29]) was purchased from Sigma-Aldrich and has a quoted minimum purity of 99.9%. For all measurements, the samples were degassed by repeated freeze–pump–thaw cycles. Comparisons of the present spectrum with those of a number of possible contaminants (O_2, CO_2, H_2O, N_2) have revealed no evidence for impurities.

4. Results and discussion

4.1 Valence excitation of C_2Cl_4

Figure 1 shows the full range of the present C_2Cl_4 spectrum. Notwithstanding the poor signal-to-noise ratio below 4.6 eV, the data provides the first photoabsorption evidence for a feature extending from <3.8 eV to 4.3 eV. The low cross section and diffuse shape of this band suggests an excitation to a dissociative state which is *optically-forbidden* on a symmetry or spin basis. Transitions of this kind can be probed more effectively in ion or electron energy loss spectroscopy (EELS) experiments. Moore [30] observed a local maximum at 4.2 eV for He^+ energy loss following 3 keV impact upon C_2Cl_4. The only EELS data available in the literature shows a band extending from 2.6 to 4.5 eV with maximum at 3.54 eV [12]. The high-energy limit of this EELS structure is consistent with the present photoabsorption feature, while the energy of the band maximum agrees with the most recently calculated value of 3.53 eV for electronic promotion from the HOMO to a π*(C=C) orbital (excitation to the 1 $^3B_{1u}$ state) [16]. While the photoabsorption cross section (5×10^{-3} Mbarn, around 10^4 times weaker than the excitation to the 1 $^3B_{1u}$ state) is

rather high for a spin-forbidden transition, Arulmozhiraja et al.'s [16] calculated vertical excitation energies are too high for the feature to be assigned to an identified singlet transition.

The calculated and experimental vertical energies of the π → π* triplet transitions of the *chlorinated ethylenes* are given in table 3 with their lowest adiabatic ionization energies (IE). A clear trend is apparent for reduced IE with increased chlorination, indicating destabilization of the HOMO. Similarly, the π → π* triplet transition generally occurs at lower energy in more chlorinated ethylenes[*]. It is interesting to note that the difference between the adiabatic IE and the EELS vertical energies [12] of this transition in chlorinated ethylenes does not show any systematic dependence on the level of chlorination. This indicates that any destabilization of the destination π*(C=C) MO due to chlorination is insignificant in comparison with that of the HOMO.

On the basis of the observed intensities of vibrational series originating at Rydberg transitions, Berry [10] estimated that valence excitations account for ≥90% of the total photoabsorption cross section of chlorinated ethylenes below 8.0 eV. Accordingly, the broad band centered at 6.202 eV in the C_2Cl_4 spectrum (figure 2) is attributed predominantly to a singlet valence transition (π → π). Contrary to the present analysis, Berry [10] also proposed unspecified *probable weaker* contributions to this band from n → π* and n → σ* singlet excitations. Arulmozhiraja et al.'s [16] recent calculations indicate that transitions of this kind contribute to the band centered at 7.67 eV.

The calculated and experimental energies of the singlet valence transitions of C_2Cl_4 are presented in table 4 and figure 2. The lowest energy *optically allowed* band in the present spectrum begins at 4.4 eV, in agreement with Lacher et al.'s [7] near-UV absorption measurement. The first discernable feature in this band appears as a shoulder centered at 5.34 eV and is tentatively assigned to a π(C=C) → σ*(C-Cl) transition in agreement with Robin [19]. It should be noted, however, that Robin [19] proposed $3p\pi_{Cl}$ as an alternative origin and π*(C=C) as a possible terminating MO. No evidence is observed for vibrational structure associated with this broad transition, suggesting prompt dissociation. Arulmozhiraja et al. [16] also reported that the lowest energy singlet transition with non-zero oscillator strength has π(C=C) → σ*(C-Cl) character (excitation to the $1\ ^1B_{1u}$ state), although the calculated vertical energy is distinctly higher than the present value.

The shoulder centered at 5.90 eV is attributed to a π(C=C) → π*(C=C) singlet transition in agreement with Dauber and Brith [11] and Robin [19]. The following shoulder at 6.07 eV is assigned to an excitation of the ν_1 mode (C=C stretch), also following the previous analysis [11]. The corresponding vibrational excitation energy (0.17 eV) is markedly lower than observed in the neutral ground state (0.195 eV). This indicates a weakening of the inter-carbon bond and increased separation of the nuclei, as expected for vacation of a bonding MO and occupation of an anti-bonding MO. The absence of features attributable to other vibrational modes, in particular ν_4 (CCl_2 twist), suggests that the molecule's planar geometry is maintained in the excited state.

Dauber and Brith [11] compared their gas-phase photoabsorption spectrum with equivalent measurements for solid C_2Cl_4 and for the molecule in a Kr matrix. The repression of the π → 3s Rydberg transition (ν_{00} at 6.24 eV) in these phases simplified the analysis, revealing an extended $n\nu_1$ series associated with the π(C=C) → π*(C=C) transition. It was suggested that the variation in the energy separations of features in this series could be attributed to anharmonicity [11]. In the present work, the possible $n\nu_1$ features above n=2 are hidden by the strong and regular vibrational structure associated with the π → 3s transition (see section 4.2). Following Dauber and Brith's [11] analysis, the present local absorption maximum at 6.202 eV is tentatively attributed to the π(C=C) → π*(C=C) transition combined with $2\nu_1$ excitation. Similarly, Koerting et al.'s [12] EELS studies showed the vertical π(C=C) → π*(C=C) transition to occur at 6.21 eV. The

[*] The most recent theoretical and experimental vertical energies for the C_2Cl_4 π → π* triplet transition follow this trend [12,16]. However the measurements and calculations reported previously by Moore [30] and Kato et al. [13] do not.

calculated vertical energies for this transition (6.46 and 6.41 eV [13,16]) are in quite good agreement with the experimental data.

The broad feature extending from 7.2 to 7.8 eV and centered at 7.670 eV has been attributed principally to excitation from a non-bonding orbital localized on the Cl atom [11,16,19]. The band maximum agrees quite closely with the vertical energies calculated by Arulmozhiraja et al. [16] for $n^- \rightarrow \sigma^*$ transitions (7.94 and 8.08 eV). However, the calculated oscillator strengths of these transitions are too weak to account for the 7.2-7.8 eV structure. Therefore, although the calculated vertical energy is distinctly higher (8.44 eV) than the present maximum (7.670 eV), we have assigned the band to the relatively strong $n_\perp(Cl) \rightarrow \pi^*(C=C)$ transition to the $3\ ^1B_{2u}$ excited state. The calculated oscillator strength of this transition is 36% of the value for the $\pi \rightarrow \pi^*$ transition [16], similar to the 44% ratio observed in the present spectrum. The poorly-resolved fine structure in this band remains largely unassigned. Unlike the $\pi(C=C) \rightarrow ns$ (see section 4.2) and $\pi(C=C) \rightarrow \pi^*(C=C)$ transitions, no clear evidence for a v_1 series is apparent. This supports associating the band with excitation from an n(Cl) orbital, as opposed to from the π(C=C) HOMO.

At energies above the $n_\perp(Cl) \rightarrow \pi^*(C=C)$ maximum, the sharp Rydberg transitions and their associated vibrational series are clearly superposed upon a broader photoabsorption band structure. Below 8.5 eV, it seems reasonable to assume that this is dominated by $n_\perp(Cl) \rightarrow \pi^*(C=C)$ band, possibly with a pre-dissociative contribution due to relaxation from Rydberg states into the $3\ ^1B_{2u}$ valence state (see table 4). At higher energies, Kato's [13] semi-empirical self consistent field theory predicted a $\pi \rightarrow \pi^*$ transition with a vertical energy of 9.23 eV and an oscillator strength ~50% of the lower-energy $\pi \rightarrow \pi^*$ band centered at 6.20 eV in the present spectrum. It seems plausible that a transition of this kind may contribute to the present spectrum close to the adiabatic ionization energy. However, Arulmozhiraja et al.'s [16] more advanced calculations (symmetry-adapted cluster configuration interaction theory) have not confirmed the possible presence of valence excited states with non-zero oscillator strengths above 8.44 eV.

4.2 Rydberg excitation of C_2Cl_4

To help assign features arising from Rydberg series, the standard equation is used:

$$E_n = E_I - (R / (n-\delta)^2) \qquad \text{[eq. 2]}$$

where E_n is the energy of the neutral excited state, E_I the ionization limit to which the series converges (this may be the ionic ground state or an ionic excited state), R the Rydberg constant (13.61 eV), n the principal quantum number, and δ the quantum defect accounting for the penetration of the Rydberg orbital into the core. Quantum defects of 0.9–1.2, ~0.7, and ~0-0.3 are expected for transitions from the C_2Cl_4 HOMO (primarily C=C localized) to ns, np, and nd orbitals, respectively [33].

4.2.1 Rydberg series converging to ionic ground state

The lowest energy Rydberg band in the present spectrum is assigned to the $\pi(C=C) \rightarrow 3s$ transition (figure 2). In agreement with Walsh [6] and with Dauber and Brith [11], the shoulder at 6.24 eV is identified as the origin of this band (the adiabatic transition). By comparing single-photon absorption with (2+1) REMPI results, Heath and Robin [34] deduced that the $\pi \rightarrow 3s$ v_{00} transition must occur in the range 6.24-6.27 eV and proposed 6.2524 eV as the most likely origin of the observed vibrational series.

The vertical energy of the $\pi \rightarrow 3s$ transition has been calculated at 6.72 eV [16] (see table 5), in reasonable agreement with the present value of 6.584 eV (the vibrational peak with the greatest cross section compared with the preceding local minimum). Arulmozhiraja et al. [16] suggested that the calculated vertical energy supports assigning the origin of the $\pi \rightarrow 3s$ transition to the feature observed by Goto [8] at 6.58 eV. We do not consider this proposed origin to be consistent

with the vibrational structure in the present spectrum. Moreover, the quantum defect for such a v_{00} transition would be 0.77, lower than expected for an excitation to an *n*s state (0.9 - 1.2 [33]).

The fine structure assigned to the π → 3s transition in the present and previous work [6,11] is summarized in table 6. Although Heath and Robin [34] did not give a detailed description of their single-photon absorption result, their interpretation of the 3s band is consistent with the present analysis. The structure is characterized by excitation of the symmetric v_1 (C=C stretch) and v_2 (C-Cl stretch) modes. The regularity of the vibrational structure and its intensity in comparison with the v_{00} feature indicate that the excited state has the same symmetry as the ground state (D_{2h}). Since s orbitals have ag symmetry in the D_{2h} group, only v_1, v_2, and v_3 vibrations can be excited strongly in this transition [9]. The average v_2 excitation energy in the π → 3s band (0.054 eV) is essentially the same as observed in the neutral electronic ground state (0.055 eV), suggesting that the HOMO has no C-Cl bonding component. Conversely, the v_1 features are separated by an average energy of 0.168 eV, in close agreement with the value in the ionic ground state (table 4 [22]) and markedly lower than that in the neutral electronic ground state. This indicates similar geometry in the $2\ ^1B_{3u}$ Rydberg state and the $^2B_{2u}$ ionic state, as well weakening of the inter-carbon bond due to the vacation of the π(C=C) HOMO.

The *one-photon-forbidden* π → *n*p_x and π → *n*f series have been explored in detail by Williams et al. [14] using two-photon resonant ionization spectroscopy. Any possible very weak evidence for these transitions in the present spectrum is hidden by the dense structure in the coinciding energy range (7.20-9.33 eV). Conversely, π → *n*d transitions are *one-photon-allowed* for C_2Cl_4. Robin [19] suggested that a π → 3d excitation may contribute to the broad band centered at 7.670 eV. Arulmozhiraja et al. [16] predicted a π → 3dσ transition with a vertical energy of 7.99 eV and oscillator strength ~15% of the π → 3s transition (see table 5). We have not been able identify this relatively weak transition with confidence in the present spectrum. Similarly, no clear photoabsorption evidence is apparent for the weak 3dπ and 3dσ excitations with calculated vertical energies at 8.17 and 8.21 eV [16].

Arulmozhiraja et al. [16] identified a π → 3dπ transition with an oscillator strength equal to that of the π → 3s transition (table 5). The calculated vertical energy (8.13 eV) of this band is close to the strongest peak (8.046 eV) of the vibrational series beginning at 7.880 eV. We have therefore attributed this band to a π → 3dπ transition, contrary to the previous π → 4s assignment [6,9]. No calculations are available to clarify Rydberg assignments with principle quantum numbers above *n* = 3. We propose a π → *n*dπ series beginning at the strong 3dπ transition, whereas Humphries et al. [9] assigned the same features to an extended π → *n*s series. Both sets of suggested assignments yield plausible quantum defects.

The fine structure associated with the π → *n*dπ transitions (*n* = 3-5) is presented in figure 3 and table 7. The similarity of these vibrational series with the π → 3s band is unsurprising when we consider that the same valence orbital is vacated in each case, while the terminating Rydberg orbitals have minimal effect on the molecular geometry. The initial nv_1 peaks are strong in comparison with the corresponding adiabatic transitions, indicating that the excited states maintain the symmetry of the neutral ground state (D_{2h}) [9] despite the evident weakening of the inter-carbon bond. As d orbitals can have ag symmetry in the D_{2h} group, strong excitation of the v_1, v_2, and v_3 vibrational modes is possible in the π → *n*dπ bands.

The fine structure between the $n_\perp$(Cl) → π*(C-C) band maximum and the adiabatic ionization energy (table 6 and figure 3) has been studied in considerable detail by Humphries et al. [9]. In addition to the series summarized in table 7, these authors identified a number of sequence bands ~0.005 eV below the relatively strong v_{00}, v_1, and v_2 excitations. Humphries et al. [9] also reported features with an average excitation energy of 0.009 eV in the bands associated here with 3dπ and 4dπ terminating orbitals. In the present spectrum, these features are either not clearly resolved or remain unassigned.

Activation of the ν_3 mode (CCl_2 scissor) is observed in the vibrational structure associated with the π(C=C) → 3dπ and 4dπ transitions (table 6). This is not surprising given that the symmetry of the mode (ag) matches that of ν_1 and ν_2, while intuitively it seems reasonable to expect some symmetric CCl_2 scissor motion to accompany the lengthening of the inter-carbon bond caused by vacation of HOMO. The ν_3 features are weak, which may explain their apparent absence from the relatively poorly-resolved π → 3s vibrational series. As is the case for ν_2, the average excitation energy of ν_3 in the 3dπ and 4dπ excited states (0.030 eV) agrees closely with the electronic ground state value (0.029 ± 0.002 eV, table 1), providing further evidence that vacation of the HOMO has little effect on the CCl_2 group. Weak and diffuse features located 0.03 eV below the 3dπ ν_{00} and $n\nu_1$ peaks are tentatively assigned to hot band and sequence band excitations of ν_3.

4.2.2 Rydberg series converging to ionic excited states

Rydberg series converging to ionic states associated with the vacation of n(Cl) orbitals are prominent in the UV spectra of chloroalkanes and therefore expected in those of chlorinated ethylenes. Accordingly, Robin [19] assigned the peaks observed at 8.971, 9.740, and 10.384 eV in the present work to transitions associated with the ionization energies reported by Lake and Thompson [22] at 11.38 , 12.18, and 12.77 eV, respectively (table 2). All these ionization energies are associated with the vacation of purely Cl-localized non-bonding orbitals, while the corresponding photoelectron bands show no clear evidence for vibrational excitations. In common with the PES and with the $n_{\perp}$(Cl) → π*(C-C) band (section 4.1), we have not been able to identify regular fine structure around the broad photoabsorption peaks observed above the adiabatic ionization energy (figure 1). To the authors' knowledge, no calculations are available for Rydberg series converging to the ionic excited states of C_2Cl_4. Therefore, with quantum defect calculations as our only guide, we cannot propose assignments for these bands with confidence.

4.3 Absolute absorption cross section and stratospheric photolysis *lifetime*

To the authors' knowledge, the only previous absolute cross sections for UV photoabsorption by C_2Cl_4 were measured by Berry [10] from 4.8 to 8.8 eV. The maximum reported in this range was 45 Mbarn* (at 6.20 eV) [10], in good agreement with the present value of 42.4 ± 2.1 Mbarn. This comparison, as well as the agreement of previous cross sections measured at the ASTRID beamline with the most precise data available in the literature (see Eden et al. [35], for example), suggests that the present C_2Cl_4 cross sections can be relied upon across the range studied.

The present absorption cross section at 10.5 eV is 53.7 ± 2.7 Mbarn, markedly greater than the corresponding photo-ionization cross section of 23 ± 4 Mbarn reported by Kanno and Tonokura [36]. This supports the interpretation that the present UV spectrum above the lowest ionization threshold (9.3256 ± 0.0006 eV [14]) is dominated by excitations to Rydberg states belonging to series converging to ionic excited states (section 3.2).

The present absolute cross section values and solar actinic flux measurements from the literature [37] have been used to calculate the atmospheric UV photolysis rates of C_2Cl_4 as a function of altitude from 20 km to the stratopause at 50 km (*UCL model* [38,39]). The reciprocal of the photolysis rate at a given altitude corresponds to the local photolysis *lifetime* (the time taken for the molecule to photo-dissociate assuming that the solar flux remains constant). The reliability of this simple model is supported by the approximate agreement of the photolysis lifetimes calculated for CF_3Cl, CF_3I, CH_2ICl, and C_2H_5I [38,40] with those generated by previous authors using more complex atmospheric models [41,42].

Short photolysis lifetimes were calculated for C_2Cl_4 at 50 km and 40 km (~10 and 15 sunlit minutes, respectively). This indicates that the molecule is destroyed efficiently by UV radiation in

* This cross section has been read from a figure [10]; to the authors' knowledge, the numerical value is not available in the literature.

the high stratosphere, releasing Cl and CCl_2 radicals (in π(C=C) → σ*(C-Cl) and π(C=C) → π*(C=C) transitions; see figure 2) which react with ozone. The local photolysis lifetime of C_2Cl_4 rises to ~1 and >10 sunlit hours at 30 and 20 km, respectively, and increases further at lower altitudes. The present photolysis lifetimes are short in comparison with the stratospheric (12-49 km) lifetime of 1.79 years calculated by Kindler et al. [1] taking into account photolysis, reactions with OH, and molecular transport. Singh et al. [2] reported that <1% of C_2Cl_4 emissions enter the stratosphere.

Photolysis rates below 20 km depend strongly on the very weak UV cross sections of C_2Cl_4 at wavelengths above 270 nm (energies below 4.6 eV, see figure 1), coinciding with large percentage errors in the present data. At these altitudes, local lifetimes depend strongly on competing pathways for the removal of the compound from the atmosphere, notably solubility in water droplets and reactions with OH and Cl radicals. Indeed, as the most abundant reactive species in the troposphere [43], OH radical driven processes have been reported to account for 98% of tropospheric C_2Cl_4 removal [2].

5. Conclusions

In response to the first *ab initio* calculations of the electronic transitions of C_2Cl_4, published recently by Arulmozhiraja et al. [16], we present a new high-resolution UV spectrum of C_2Cl_4. The valence and Rydberg assignments below 8.5 eV are in good agreement with the theoretical calculations but differ from earlier interpretations with respect to several transitions. In particular, an *n*dπ series is proposed to account for Rydberg bands between 7.8 and 9.0 eV, contrary to Humphries et al.'s *n*s assignments [9]. The present identification of vibrational structure associated with excitations from the HOMO, however, agrees closely with the previous spectroscopic studies. Due to the lack of comparable calculations and clear vibrational series in the high-energy part of the spectrum, specific assignments have not been proposed for the bands between 9.0 - 10.8 eV corresponding to Rydberg transitions from n(Cl) MOs.

The present work provides the first photoabsorption evidence for a very weak feature extending from <3.8 eV to 4.3 eV which is provisionally attributed to a π(C=C) → π*(C=C) transition to the $1\,^3B_{1u}$ dissociative state [16]. This result highlights the necessity for a more sensitive (higher pressure and / or path length) photoabsorption cross section measurement over the full range of the transition indicated by previous EELS measurements (2.6-4.5 eV) [12] since even very weak absorption in this energy range can have a significant effect on solar photolysis rates at altitudes below 20 km.

The present absolute photoabsorption cross sections of C_2Cl_4 are the first measured over the full energy range 3.8-10.8 eV (325-115 nm). This data has been used to calculate approximate UV photolysis *lifetimes* of this aeronomic molecule in the mid- to upper stratosphere (20-50 km). The calculated photolysis lifetimes of C_2Cl_4 are short (ranging from minutes to 10s of sunlit hours) at these altitudes, leading to CCl_2 and Cl radical production.

Acknowledgements

The authors wish to acknowledge the European Commission for access to the ASTRID facility at the University of Aarhus, Denmark and the support from the European Commission for access to research infrastructure action of the improving human potential program. S.E., N.J.M., and P.L.V. acknowledge the support from the British Council for the Portuguese-English joint collaboration. S.E. acknowledges the support of the British EPSRC through the Life Sciences Interface Fellowship program and of the European Commission through a Marie Curie Intra-European Reintegration Grant. PLV acknowledges the visiting fellow position at the Department of Physics and Astronomy, The Open University, UK.

References

[1] T.P. Kindler, W.L. Chameides, P.H. Wine, D.M. Cunnol, and F.N. Alyea, *J. Geophys. Res.* 100 (D1) (1995) 1235.
[2] H.B. Singh, A.N. Thakur, and Y.E. Chen, *Geophys. Res. Lett.* 23 (1996) 1529.
[3] E.P. Olaguer, *Environ. Sci. Poll. Res.* 9 (2002) 175.
[4] I.J. Simpson, S. Meinardi, N.J. Blake, F.S. Rowland, and D.R. Blake, *J. Geophys. Res. Lett.* 31 (2004) L08108.
[5] N.J. Blake, D.R. Blake, I.J. Simpson, S. Meinardi, A.L. Swanson, J.P. Lopez, A.S. Katzenstein, B. Barletta, T. Shirai, E. Atlas, G. Sachse, M. Avery, S. Vay, H.E. Fuelberg, C.M. Kiley, K. Kita, F.S. Rowland, *J. Geophys. Res. - Atmospheres* 108 (2003) 8806.
[6] D. Walsh, *Trans. Faraday Soc.* 41 (1945) 35
[7] J.R. Lacher, L.E. Hummel, E.F. Bohmfalk, and J.D. Park, *J. Am. Chem. Soc.* 72 (1950) 5486.
[8] K. Goto, Sci. *Light* 9 (1960) 104
[9] M. Humphries, A.D. Walsh, and P. A. Warsop, *Trans. Faraday Soc.* 63 (1967) 513.
[10] M.J. Berry, *J. Chem. Phys.* 61 (1974) 3114.
[11] P. Dauber and M. Brith, *Chem. Phys.* 11 (1975) 143.
[12] C.F. Koerting, K.N. Walzl, and A. Kuppermann, *J. Chem. Phys.* 109 (1984) 140.
[13] H. Kato, H. Hirao, H. Konishi, and T. Yonezawa, *Bull. Chem. Soc. Japan* 44 (1971) 2062.
[14] A. Williams, T.A. Cool, and C.M. Rohlfing, *J. Chem. Phys.* 93 (1990) 1521.
[15] A. Williams and T.A. Cool, *J. Phys. Chem.* 97 (1993) 1270.
[16] S. Arulmozhiraja, M. Ehara, and H. Nakatsuji, *J. Chem. Phys.* 129 (2008) 174506.
[17] K. Takeshita, J. Chem. Phys. 102 (1995) 8922.
[18] S. Eden, P. Limão-Vieira, P. Kendall, N.J. Mason, J. Delwiche, M.-J. Hubin-Franskin, T. Tanaka, M. Kitajima, H. Tanaka, H. Cho, and S.V. Hoffmann *Chem. Phys.* 297 (2004) 257.
[19] M.B. Robin, *Higher Excited States of Polyatomic Molecules* (Academic, New York, 1975 and 1985), Vols. II and III.
[20] K. Kimura, S. Katsumata, Y. Achiba, T. Yamazaki, and S. Iwata, *Handbook of He(I) Photoelectron Spectra of Fundamental Organic Molecules*, Japan Scientific Societies Press, Tokyo (1981).
[21] T. Shimanouchi, *Tables of Molecular Vibrational Frequencies Consolidated Volume I*, National Bureau of Standards (1972) 1-160.
[22] R.F. Lake and H. Thompson, *Proc. R. Soc. London Ser. A* 315 (1970) 323.
[23] S.G. Lias, "Ionization Energy Evaluation" in *NIST Chemistry WebBook*, NIST Standard Reference Database Number 69, Eds. P.J. Linstrom and W.G. Mallard, National Institute of Standards and Technology, Gaithersburg MD, 20899, http://webbook.nist.gov, (retrieved February 2, 2009).
[24] J.S. Shapiro and F.P. Lossing, *J. Phys. Chem.* 72 (1968) 1552.
[25] S. Eden, P. Limão-Vieira, S.V. Hoffmann, and N.J. Mason, *Chem. Phys.* 323 (2006) 313.
[26] C. Vandaele, P.C. Simon, J.M. Guilmot, M. Carleer, and R. Colin, *J. Geophys. Res. - Atmospheres* 99 (D12) (1994) 25599.
[27] D.E. Freeman, K. Yoshino, J.R. Esmond, W.H. Parkinson, *Planet. Space Sci.* 32 (1984) 1125.
[28] A. Giuliani, J. Delwiche, S.V. Hoffmann, P. Limão-Vieira, N.J. Mason, and M.-J. Hubin-Franskin, *J. Chem. Phys.* 119(7) (2003) 3670.
[29] *NIST Chemistry WebBook* 2009 http://webbook.nist.gov
[30] J.H. Moore, J. Phys. Chem. 76 (1972) 1130.
[31] R.J. Buenker, S.D. Peyerimhoff, and W.E. Kammer, *J. Chem. Phys.* 53 (1971) 814.
[32] A. Kuppermann, W.M. Flicker, and O.A. Mosher, *Chem. Rev.* 79 (1979) 77.
[33] C. Sandorfy (Ed.), *The Role of Rydberg States in Spectroscopy and Photochemistry*, Kluwer Academic Publishers, Dordrecht (1999).
[34] A. Heath and M.B. Robin, *J. Am. Chem. Soc.* 102 (1980) 1796.
[35] S. Eden, P. Limão-Vieira, S.V. Hoffmann, and N.J. Mason, *Chem. Phys.* 331 (2007) 232.
[36] N. Kanno and K. Tonokura, *Applied Spectroscopy* 61 (2007) 896.
[37] W.B. Demore, S.P. Sandler, D.M. Golden, R.F. Hampson, M.J. Kurylo, C.J. Howard, A.R. Ravishankara, C.E. Kolb, and M.J. Molina, *Chemical Kinetics and Photochemical Data for*

Use in Stratospheric Modelling, Evaluation Number 12, Jet Propulsion Laboratory Publication 97-4 (1997).
[38] P.A. Kendall, *Spectroscopic Studies of Molecules Related to Global Warming*, University of London PhD Thesis (2003).
[39] P. Limão-Vieira, S. Eden, P.A. Kendall, N.J. Mason, and S.V. Hoffmann, *Chem. Phys. Lett.* 364 (2002) 535.
[40] S. Eden, *Spectroscopic and Electron Impact Studies of Molecules Relevant to Plasma Etching*, University of London PhD Thesis (2003).
[41] P.C. Simon, D. Gillotay, N. Vanlaethem-Meuree, and J. Wisemberg, *Journal of Atmospheric Chemistry* 7 (1988) 107.
[42] O.V. Rattigan, D.E. Shallcross, and R.A. Cox, *J. Chem. Soc. Faraday Trans.* 93 (1997) 2839.
[43] C. Trudell and S.J.W. Price, *Can. J. Chem.* 57 (1979) 2256.

Figure Captions

Figure 1: Full UV absorption spectrum of C_2Cl_4 recorded at the University of Aarhus
Figure 2: C_2Cl_4 absorption cross section in the range 4.5 – 8.0 eV
Figure 3: C_2Cl_4 absorption cross section in the range 7.8 – 9.4 eV

Table Captions

Table 1: Ground state vibrational energy levels [21]
Table 2: Summary the lowest ionic states of C_2Cl_4
Table 3: Ionization energies and $\pi \rightarrow \pi^*$ triplet transitions of ethylene and c*hlorinated ethylenes*
Table 4: Singlet valence transitions of C_2Cl_4
Table 5: Singlet Rydberg transitions of C_2Cl_4
Table 6: Vibrational structure (ν_1 and ν_2) associated with the $\pi \rightarrow 3s$ transition
Table 7: Vibrational structure in the range 7.75 – 9.1 eV associated with Rydberg transitions from the HOMO (π) to *n*dπ orbitals.

Table 1: Ground state vibrational energy levels [21]

Mode	Description	Symmetry	Energy (eV)	Error
v_1	C=C stretch	ag	0.195	± 0.002
v_2	CCl_2 s-stretch	ag	0.055	± 0.002
v_3	CCl_2 scissor	ag	0.029	± 0.002
v_4	CCl_2 twist	au	0.014	± 0.004
v_5	CCl_2 a-stretch	b_1g	0.124	± 0.002
v_6	CCl_2 rock	b_1g	0.043	± 0.002
v_7	CCl_2 wag	b_1u	0.036	± 0.002
v_8	CCl_2 wag	b_2g	0.063	± 0.002
v_9	CCl_2 a-stretch	b_2u	0.113	± 0.001
v_{10}	CCl_2 rock	b_2u	0.022	± 0.001
v_{12}	CCl_2 s-stretch	b_3u	0.096	± 0.001
v_{13}	CCl_2 scissor	b_3u	0.038	± 0.001

Table 2: Summary the lowest ionic states of C_2Cl_4

Photoelectron experiments			SDCI* calculations [17]			Character of the vacated MO		Ionic state vibration [22]	
[20]	[22]							Activation energy (eV)	mode
VIE† (eV)	VIE† (eV)	AIE† (eV)	VIE† (eV)	AIE† (eV)	Ionic state	[20]	[22]		
9.51	9.51	9.34	9.23	8.81	$^2B_{2u}$	π(C=C), n(Cl) #	π(C=C)	0.164	ν_1
								0.060-0.044	ν_2
11.37	11.38	-	11.49	11.48	$^2B_{2g}$	n(Cl)	n(Cl)	-	-
12.19	12.18	-	12.40	12.40	^2A_u			-	-
-	12.44	-						-	-
12.58	12.54	-	12.53	12.30	$^2B_{3u}$			-	-
-	12.67	-	12.77	12.76	$^2B_{1g}$			-	-
-	12.77	-	12.88	12.61	$^2B_{1u}$			-	-
-	12.91	-	13.11	13.01	^2A_g			-	-
13.51	13.48	-	13.72	13.64	$^2B_{3g}$		n(Cl), π(C=C)	0.057	ν_2
14.67	14.68	-	-	-	-	σ(C-Cl)	-	-	-
15.12	15.10	-	-	-	-	n(Cl), π(C=C)	-	-	-
16.78	16.73	-	-	-	-	σ(C-Cl)	-	-	-
-	18.31	-	-	-	-	σ(C-C)	-	-	-

* Single and double excitation configuration interaction
† VIE and AIE = Vertical and adiabatic ionization energies, respectively
# Kimura et al.'s [20] suggestion that the HOMO has partial n(Cl) character is in agreement with Robin [19].
Note that this table only summarizes a selection of the C_2Cl_4 ionic state studies in the literature [29].

Table 3: Ionization energies and π → π* triplet transitions of ethylene and *chlorinated ethylenes*

Vertical transition [†] π(C=C) → π*(C=C) singlet to triplet	Energy (eV)				
	C_2H_4	C_2H_3Cl	$C_2H_2Cl_2$ [#]	C_2HCl_3	C_2Cl_4
EELS [12]	4.32 [‡]	4.13 (3.4-5.1)	3.75 (3.2-5.1) [1,1] 3.94 (3.0-5.2) [1,2 Z] 3.84 (2.9-4.8) [1,2 E]	3.70 (3.0-4.7)	3.54 (2.6-4.5)
3 keV He^+ impact energy loss [§] [30]	4.3	4.0	3.9 [1,1]	-	4.2
Photoabsorption (present work)	-	-	-	-	(<3.8 - 4.3) [?] [W]
Theoretical [31]	4.26	-	-	-	-
Theoretical [13]	-	4.17	3.95 [1,1] 3.82 [1,2 Z] 3.81 [1,2 E]	3.99	4.38
Theoretical [16]	-	-	4.00 [1,2 Z] 3.97 [1,2 E]	-	3.53 ($1\,^3B_{1u}$)
Adiabatic IE [23] π(C=C)	10.5138 ± 0.0006	9.99 ± 0.02	9.81 ± 0.04 [1,1] 9.66 ± 0.01 [1,2 Z] 9.64 ± 0.02 [1,2 E]	9.46 ± 0.02	9.326 ± 0.001
IE [23] – vertical (π→ π*) [12]	6.19	5.86	6.06 [1,1] 5.72 [1,2 Z] 5.8 [1,2 E]	5.76	5.79

[#] Isomer specified in square brackets.
[†] Full range of the band given in brackets, when available.
[‡] Kuppermann et al. [32]
[§] Resolution 0.35 eV
[?] Due to the poor signal-to-noise ratio and the low-energy cut-off at 3.8 eV in the present data, the vertical position of this band is uncertain and its assignment should be considered as provisional.
[W] Very weak and diffuse

Table 4: Singlet valence transitions of C_2Cl_4

SCF MO[#] calculations [13]			SAC-CI* calculations [16]				Previous experiments		Present work		
Energy (eV)	Transition character	Oscillator strength[‡]	Energy (eV)	Excited state	Transition character	Oscillator strength[‡]	Energy (eV)	Reference	Energy (eV)	Maximum [†] cross section (Mbarn) ± 5%	Transition character
-	-	-	6.30 [V]	$1\,^1B_{3u}$	$\pi \rightarrow \sigma^*_0$	0.0004	5.39 [V]	Berry [10]	5.34 [D V]	-	$\pi(C{=}C) \rightarrow \sigma^*(C\text{-}Cl)$
-	-	-	-	-	-	-	5.90 [A]	Dauber and Brith [11]	5.90 [D A]	-	$\pi(C{=}C) \rightarrow \pi^*(C{=}C)$
-	-	-	-	-	-	-	6.06		6.08 [D]	-	v_1
6.46 [V]	$\pi \rightarrow \pi^*$	1.074	6.41 [V]	$1\,^1B_{1u}$	$\pi \rightarrow \pi^*$	0.4973	6.20 [V]		6.202 [V]	42.5	$2v_1$ (?)
7.17 [V]	$n^- \rightarrow \sigma^*$	0.837	7.94 [V]	$1\,^1B_{2u}$	$n^- \rightarrow \sigma^*_-$	0.0092	7.67 [V]	Dauber and Brith [11]	7.670 [V]	18.8	$n_\perp(Cl) \rightarrow \pi^*(C\text{-}C)$
-	-	-	8.08 [V]	$2\,^1B_{1u}$	$n^- \rightarrow \sigma^*_+$	0.0018					
-	-	-	8.44 [V]	$3\,^1B_{2u}$	$n_\perp \rightarrow \pi^*$	0.1785					
9.23 [V]	$\pi \rightarrow \pi^*$	0.575	-	-	-	-	-	-	-	-	-

[#] Semi-empirical self consistent field theory
* Symmetry-adapted cluster configuration interaction theory
[‡] Only transitions with non-zero calculated oscillator strengths are included in this table
[V] Vertical energy for the electronic transition
[A] Adiabatic energy
[†] Only for peaks
[D] Diffuse feature (given to lower energy precision)
(?) Uncertain assignment
In the range 3.8 - 7.75 eV, the weak and diffuse vibronic features observed at 7.32, 7.35, 7.45, 7.48, 7.51, 7.55, 7.60, 7.63, 7.65, and 7.69 eV remain unassigned.

Table 5: Singlet Rydberg transitions of C_2Cl_4

SAC-CI* calculations [16]				Present work	
Energy (eV)	Excited state	Transition character	Oscillator strength	Energy (eV)	Quantum defect
-	-	-	-	6.24 [D A]	0.90
6.72 [V]	$2\,^1B_{3u}$	π → 3s	0.0171	6.584 [V]	-
7.99 [V]	$3\,^1B_{3u}$	π → 3dσ	0.0025	-	-
-	-	-	-	7.880 [A]	- 0.07
8.13 [V]	$2\,^1B_{2u}$	π → 3dπ	0.0171	8.046 [V]	-
8.17 [V]	$3\,^1B_{1u}$	π → 3dπ	0.0002	-	-
8.21 [V]	$4\,^1B_{3u}$	π → 3dσ	0.0005	-	-

* Symmetry-adapted cluster configuration interaction theory; only transitions with non-zero calculated oscillator strengths are included in this table
[V] Vertical energy for the electronic transition
[A] Adiabatic energy
[D] Diffuse feature (given to lower energy precision)

Table 6: Vibrational structure (v_1 and v_2) associated with the π → 3s transition

Energy (eV)			Present assignment *	Quantum defect	Energy separation (eV)	
Previous work		Present work				
Walsh [6]	Dauber and Brith [11]				v_1	v_2
6.24 [A]	6.246	6.24 [D]	3s, v_{00}	0.90	-	-
6.298	6.300	6.303	v_2	-	-	0.06
6.357	6.348	6.361	$2v_2$	-	-	0.06
6.415	6.414	6.414	v_1	-	0.17	-
6.470	6.464	6.468	$v_1 + v_2$	-	-	0.054
6.527	6.515	6.526	$v_1 + 2v_2$	-	-	0.058
6.587	6.584	6.584 [V]	$2v_1$	-	0.170	-
6.636	6.630	6.64 [D]	$2v_1 + v_2$	-	-	0.06
6.698	6.684	6.69 [D]	$2v_1 + 2v_2$	-	-	0.05
6.752	6.746	6.753	$3v_1$	-	0.169	-
-	6.797	6.80 [D]	$3v_1 + v_2$	-	-	0.05
-	6.850	6.85 [D]	$3v_1 + 2v_2$	-	-	0.05
6.914	6.915	6.919	$4v_1$	-	0.166	-
-	6.965	6.97 [D]	$4v_1 + v_2$	-	-	0.05
-	7.013	7.02 [D]	$4v_1 + 2v_2$	-	-	0.05
7.081	7.073	7.081	$5v_1$	-	0.162	-
-	7.126	7.13 [D]	$5v_1 + v_2$	-	-	0.05
-	7.175	7.18 [D]	$5v_1 + 2v_2$	-	-	0.05
7.252	7.251	7.251	$6v_1$	-	0.170	-
-	7.280	7.285	*unassigned* [†]	-	-	-
7.414	7.433	7.420	$7v_1$	-	0.169	-

* In general agreement with the previous work [6,8,9,11]
[A] Walsh [6] reported this transition to be "obscured around" 6.24 eV.
[D] Diffuse feature (given to lower energy precision)
[V] Vertical energy for the electronic transition
[†] Contrary to the previous work [11], this feature is not assigned to the π → 3s vibronic series in the present work.

Table 7: Vibrational structure in the range 7.75 – 9.1 eV associated with Rydberg transitions from the HOMO (π) to *n*dπ orbitals.

Energy (eV)				Present Assignment *	Quantum defect	Energy separation (eV)			
Previous work			Present work			ν_1	ν_2	ν_3	$\nu_{3\text{-}0}$
Walsh [6]	Goto [8]	Humphries et al. [9] [§]							
-	-	-	7.85 [D]	$\nu_{3\text{-}0}$	-	-	-	-	0.03
7.880	7.880	7.882	7.880	3dπ, ν_{00} (4s) *	- 0.07 (0.93 for 4s)	-	-	-	-
7.912	-	7.914	7.910	ν_3	-	-	-	0.030	-
7.939	7.939	7.942	7.938	ν_2	-	-	0.058	-	-
-	-	7.973	7.968	$\nu_2 + \nu_3$	-	-	-	0.030	-
-	-	8.000	7.996	$2\nu_2$	-	-	0.058	-	-
-	-	-	8.02 [D]	$\nu_{3\text{-}0} + \nu_1$	-	-	-	-	0.03
8.047	8.047	8.049	8.046 [V]	ν_1	-	0.166	-	-	-
8.080	8.080	8.080	8.077	$\nu_1 + \nu_3$	-	-	-	0.031	-
8.108	8.108	8.108	8.106	$\nu_1 + \nu_2$	-	-	0.060	-	-
-	-	8.141	8.13 [D]	$\nu_1 + \nu_2 + \nu_3$	-	-	-	0.02	-
8.160	8.160	8.167	8.165	$\nu_1 + 2\nu_2$	-	-	0.059	-	-
-	-	-	8.18 [D]	$\nu_{3\text{-}0} + 2\nu_1$	-	-	-	-	0.03
8.213	8.212	8.213	8.214	$2\nu_1$	-	0.168	-	-	-
-	-	8.244	8.244	$2\nu_1 + \nu_3$	-	-	-	0.03	-
8.273	8.273	8.273	8.271	$2\nu_1 + \nu_2$	-	-	0.057	-	-
-	-	8.306	8.302	$2\nu_1 + \nu_2 + \nu_3$	-	-	-	0.031	-
8.333	8.333	8.333	8.332	$2\nu_1 + 2\nu_2$	-	-	0.061	-	-
-	-	-	8.35 [D]	$\nu_{3\text{-}0} + 3\nu_1$	-	-	-	-	0.03
8.379	8.379	8.377	8.377	$3\nu_1$	-	0.163	-	-	-
8.404	8.405	8.408	8.406	$3\nu_1 + \nu_3$	-	-	-	0.029	-
8.441	8.441	8.437	8.434	$3\nu_1 + \nu_2$	-	-	0.057	-	-
-	-	8.469	8.466	$3\nu_1 + \nu_2 + \nu_3$	-	-	-	0.032	-
8.496	8.496	8.497	8.49 [D]	$3\nu_1 + 2\nu_2$	-	-	0.06	-	-
8.544	8.544	8.540	8.539	$4\nu_1$	-	0.162	-	-	-
8.60 [D]	8.595	8.599	-	-	-	-	0.06	-	-
-	-	8.523	8.521	4dπ, ν_{00} (5s) *	- 0.11 (0.89 for 5s)	-	-	-	-
-	-	-	8.55 [D]	ν_3	-	-	-	0.03	-
-	-	8.582	8.577	ν_2	-	-	0.056	-	-
-	-	8.612	8.61 [D]	$\nu_2 + \nu_3$	-	-		0.03	-
-	-	8.643	8.637	$2\nu_2$	-	-	0.060	-	-
-	-	8.691	8.688 [V]	ν_1	-	0.167	-	-	-
-	-	8.724	8.719	$\nu_1 + \nu_3$	-	-	-	0.031	-
-	-	8.751	8.747	$\nu_1 + \nu_2$	-	-	0.059	-	-
-	-	8.783	8.778	$\nu_1 + \nu_2 + \nu_3$	-	-	-	0.031	-
-	-	-	8.806 [R]	$\nu_1 + 2\nu_2$	-	-	0.059	-	-
-	-	8.859	8.853	$2\nu_1$	-	0.165	-	-	-
-	-	-	8.885	$2\nu_1 + \nu_3$	-	-	-	0.032	-
-	-	8.921	8.913	$2\nu_1 + \nu_2$	-	-	0.060	-	-
-	-	-	8.94 [D]	$2\nu_1 + \nu_2 + \nu_3$	-	-	-	0.03	-
-	-	-	8.96 [D]	$2\nu_1 + 2\nu_2$	-	-	0.05	-	-
-	-	9.024	9.020	$3\nu_1$	-	0.167	-	-	-
-	-	-	9.06 [D]	$3\nu_1 + \nu_3$	-	-	-	0.04	-
-	-	-	9.08 [D]	$3\nu_1 + \nu_2$	-	-	0.06	-	-
-	-	8.810	8.806	5dπ, ν_{00} (6s) *	- 0.12 (0.88 for 6s)	-	-	-	-
-	-	8.978	8.971 [V]	ν_1	-	0.165	-	-	-

* The vibrational structure is identified in close agreement with Walsh [6] and Humphries et al. [9]. Contrary to the previous 4s assignment [6,9], the 7.880 ν_{00} peak is associated with a 3dπ terminating orbital following Arulmozhiraja et al.'s [16] calculations. The 4dπ and 5dπ assignments are tentative.

[D] Diffuse feature (given to lower energy precision)

[§] Humphries et al. [9] identified a number of further peaks at energies above (average difference 0.009 eV) and below (average difference 0.005 eV) the ν_{00}, ν_1, and ν_2 excitations.

[V] Vertical energy for the electronic transition

[R] This feature coincides with the proposed 5dπ ν_{00} transition.

The weak features observed at 7.79, 7.82, 7.89, 7.95, 8.06, 8.12, 8.22, 8.28, and 8.66 eV remain unassigned.

Figure 1: Full UV absorption spectrum of C_2Cl_4 recorded at the University of Aarhus

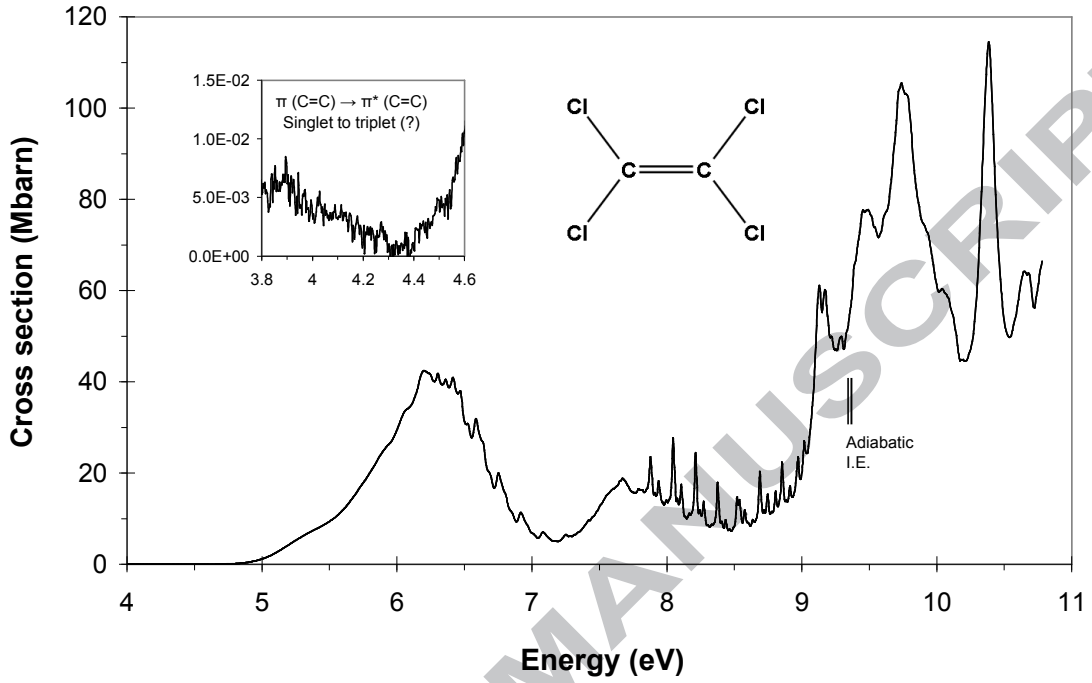

Figure 2: C_2Cl_4 absorption cross section in the range 4.5 – 8.0 eV

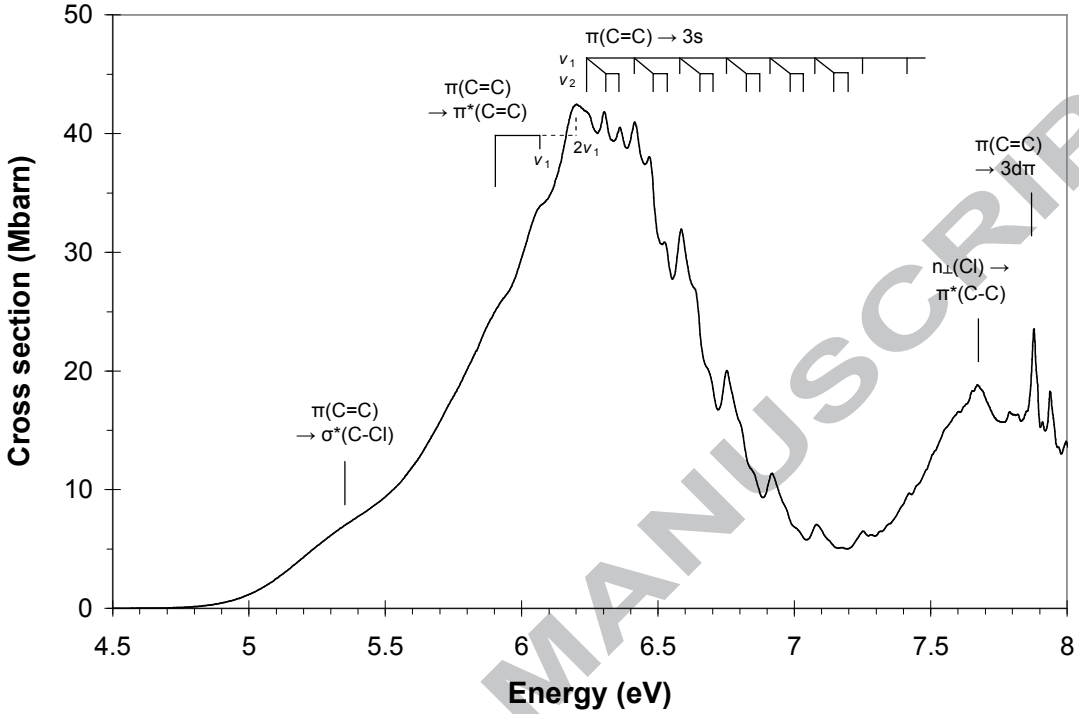

Figure 3: C_2Cl_4 absorption cross section in the range 7.8 – 9.4 eV